Forest Ecology and Management 472 (2020) 118243

Contents lists available at ScienceDirect

Forest Ecology and Management

journal homepage: www.elsevier.com/locate/foreco

Satellite observations of forest resilience to hurricanes along the northern Gulf of Mexico

Chengcheng Gang[a,b,c,*], Shufen Pan[c], Hanqin Tian[c], Zhuonan Wang[c], Rongting Xu[c], Zihao Bian[c], Naiqing Pan[c], Yuanzhi Yao[c], Hao Shi[c]

[a] Institute of Soil and Water Conservation, Northwest A&F University, Yangling 712100, China
[b] Institute of Soil and Water Conservation, Chinese Academy of Sciences and Ministry of Water Resources, Yangling 712100, China
[c] International Center for Climate and Global Change Research, School of Forestry & Wildlife Sciences, Auburn University, Auburn 36845, USA

ARTICLE INFO

Keywords:
Hurricane disturbance
Forest resilience
Vegetation index
NDII
Vegetation recovery

ABSTRACT

As one of the most destructive natural disasters, hurricanes pose a great threat to forest ecosystems, particularly in the coastal areas. A better understanding of forest resilience to hurricane disturbances is essential for reducing hazard risks as well as sustaining forests in a time of increasing climate disasters. Although hurricane-induced forest damage has been extensively studied at both local and regional levels, the lack of large-scale assessment of post-hurricane recovery still limits our understanding of forest resilience to hurricane disturbances. In this study, we utilized four remotely sensed vegetation indices (VIs), including the normalized difference infrared index (NDII), enhanced vegetation index (EVI), leaf area index (LAI), and solar-induced chlorophyll fluorescence (SIF), to examine the forest resilience to hurricanes of different strengths by quantifying the resistance, net change, and recovery of the forest after hurricanes that made landfall along the northern Gulf of Mexico from 2001 to 2015. The results revealed that the NDII was superior in monitoring the large-scale forest resilience. SIF exhibited a performance similar to that of the EVI. Wind speed was found to be the leading factor affecting forest damage and post-hurricane recovery. The impacted forest canopy began to recover approximately one month after the landfall. Woody wetlands exhibited less VI reduction and shorter recovery time than evergreen forests for the same category of hurricanes. For regions dominated by evergreen forests, NDII values lower than the multi-year average were observed across all seasons during the year after being impacted by a major hurricane. The widespread drought of 2006/2007 has aggravated the VI decrease and substantially extended the recovery period after hurricanes Ivan and Katrina. Overall, our findings derived from satellite observations provide essential information for understanding forest resilience to hurricanes as well as implementing efficient post-hurricane forest restoration.

1. Introduction

Hurricanes, one of the most powerful and destructive climate disasters, pose great threats to both human and natural systems, especially along the coastal regions of the United States (Wang et al., 2010; Wang and D'Sa, 2010). The 2005 Atlantic hurricane season is considered to be a record-breaker in terms of the intensity and frequency of hurricanes as well as the catastrophic total damage of US$74 billion (Weinkle et al., 2018; Beven et al., 2008). Terrestrial ecosystems, especially forests, are deemed most vulnerable to frequent hurricane damage, particularly along the Gulf of Mexico (McNulty, 2002; Negrón-Juárez et al., 2014; Wang and D'Sa, 2010). The substantial impacts of hurricanes on forests include defoliation, the bending or breaking of branches, and the blowdown or even uprooting of entire trees (Boose et al., 1994, 2004). The intensity of these impacts usually depends on biotic and abiotic factors, such as wind strength, topography, forest type, forest density, and the distance of the forest from the hurricane track (Dahal et al., 2015; McNulty, 2002). Alterations of the composition and structure of coastal ecosystems resulting from hurricanes definitely affect the carbon and nitrogen cycles at the landscape and regional scales, owing to powerful winds, heavy rainfall, and subsequent flooding (McNulty, 2002; Chambers et al., 2007). From 1850 to 2000, hurricanes caused carbon release from the continental U.S. forests at the rate of 29 Tg/yr (Zeng et al., 2009). In 2005, Hurricane Katrina alone produced 105 Tg of carbon emissions, the magnitude of which is comparable to the total U.S. forest carbon sink (Chambers et al., 2007).

* Corresponding author at: Institute of Soil and Water Conservation, Northwest A&F University, Yangling 712100, China.
E-mail address: gangcc@ms.iswc.ac.cn (C. Gang).

https://doi.org/10.1016/j.foreco.2020.118243
Received 29 March 2020; Received in revised form 30 April 2020; Accepted 13 May 2020

In addition, the hurricane-driven flooding events cause an intrusion of salty water into coastal wetlands and inland watersheds, which can destroy marsh vegetation and increase release of greenhouse gases (Vidon et al., 2017; Wang and D'Sa, 2010).

The timely and accurate identification of post-hurricane damage is essential for the ability of land managers and government officials to take immediate protection and to guide the post-hurricane restoration (Stanturf et al., 2007; Wang et al., 2010; Wang and D'Sa, 2010). The existing estimation of post-hurricane impacts generally includes ground observation and remote sensing-based methods. Ground or aerial surveys can provide detailed information on forest damage along the track of hurricanes (Boutet and Weishampel, 2003; Chambers et al., 2007; Imbert, 2018). However, field observation-based studies are often constrained to small spatial scales due to the limited forest inventory plots and the resources consumed. The development of remote sensing technology has facilitated the quantification of post-hurricane damage at extended spatial and temporal scales (Dahal et al., 2015; Hu and Smith, 2018; Wang and D'Sa, 2010; Zeng et al., 2009). The Moderate Resolution Imaging Spectroradiometer (MODIS) products have frequently been used to assess of hurricane damage (Dahal et al., 2015; de Beurs et al., 2019; Negrón-Juárez et al., 2014; Potter, 2014; Wang et al., 2010; Wang and D'Sa, 2010). Vegetation indices, such as the normalized difference vegetation index (NDVI) (Ayala-Silva and Twumasi, 2004; Ramsey et al., 1998, 2001), enhanced vegetation index (EVI) (Rogan et al., 2011; Wang and D'Sa, 2010), tasseled cap water index (TCWI) (Mostafiz and Chang 2018), normalized difference infrared index (NDII) (Aosier et al., 2007; Dahal et al., 2015; Wang et al., 2010), are widely used to detect the forest canopy change by comparing the difference between pre- and post-hurricane status. In addition, Potter (2014) performed a global analysis concerning the damage to coastal ecosystem vegetation resulting from tropical storms between 2006 and 2012 based on a MODIS quarterly indicator of cover change. Most of these extensive studies, however, were narrowly focused on a single event or were based on a single indicator. In order to accurately quantify forest resilience to hurricane disturbances, as well as satellite-observational uncertainties, it is important to use multiple indicators and detect their performances on hurricanes of different intensities.

Compared with the large amount of research focusing on the assessment of post-hurricane forest damage, the trajectory of recovery has received less attention. Ground surveys of post-hurricane recovery are conducted by comparing the composition and physical parameters of trees pre- and post- hurricane (Burslem et al., 2000; Imbert, 2018). The lack of long-term post-disturbance data has made it difficult in monitoring the recruitment process of forests at a larger spatial scale (Bellingham et al., 1995; Burslem et al., 2000). Imbert (2018) found that mangroves in inner, tall-canopy stands need 23 years to recover from a hurricane disturbance, while the fringe and scrub stands require even more time. Satellite monitoring facilitates capturing the damage extent and the long-term pattern of forest recovery at large spatial scales. Wang and D'Sa (2010) assessed the utility of MODIS EVI in detecting the forest damage and monitoring the forest recovery after hurricanes Katrina, Rita, Ike, and Lili. de Beurs et al. (2019) developed a MODIS-based disturbance index to detect the damage from hurricane and drought on four major Caribbean islands since 2001. These efforts have improved our understanding concerning the post-hurricane recovery of forests, but it is still unclear how long a forest needs to recover from the damage induced by hurricanes, or whether different forest types have varied recovery speeds.

The frequent hurricanes in the Gulf of Mexico have repeatedly exposed the forests to strong winds, floods, heavy rain, landslides, and storm surges (Chapman et al., 2008; Wang and D'Sa, 2010). More than 250 hurricanes have struck the northern Gulf of Mexico since 1851, and nearly one-third of them were categorized as major hurricanes (Blake et al., 2005). The coastal areas of the southern U.S. will be exposed to a greater risk of hurricanes over the next 40 years (Stanturf et al., 2007). Therefore, in order to better understand the impacts of hurricanes on forests, we quantified the forest resilience to hurricanes that made landfall along the northern Gulf of Mexico from 2000 to 2015 through the utilization of four remotely sensed vegetation indices (VIs), including the NDII, EVI, LAI, and solar-induced chlorophyll fluorescence (SIF). Specifically, the objectives of this study were to: (1) quantify the resistance (how much a VI changes during a hurricane) and net change (how much the VI changed compared to the state before hurricane) of forest after each hurricane over the study period; (2) estimate the seasonal and interannual variations of VIs during the post-hurricane period; and (3) assess how long the damaged forests take to recover from a hurricane event and determine the potential influencing factors. By comparing the results among the four VIs, we also attempted to identify an optimal indicator for characterizing the post-hurricane damage and recovery trajectory of forests.

2. Methods and data sources

2.1. Hurricane data

The best tracks for hurricanes that made landfall along the northern Gulf of Mexico during 2001–2015 were extracted from the National Hurricane Center (NHC) data archive (https://www.nhc.noaa.gov/data/). NHC, which is a component of the National Centers for Environmental Prediction (NCEP), archives hurricane track database including location, central pressure, and maximum wind speed of tropical cyclones since 1851 (Dahal et al., 2015; Landsea and Franklin, 2013). During the period 2001–2005, 13 hurricanes made landfall along the northern Gulf of Mexico (Table 1). It is worth noting that the Hurricane Katrina made three landfalls in 2005. The first landfall was in Florida as a Category 1 hurricane, while the second and third landfalls were in Louisiana and near the Louisiana-Mississippi border, respectively, as a Category 3 hurricane (Fig. 1). In the present study, the post-hurricane damage of first landfall of Katrina was counted separately because of its intensity and the long distance from the second and third landfalls. In addition, as the NDII, EVI, LAI, and SIF data are available from 2001 to 2015, the aftermath of Hurricane Lili, which hit Louisiana as a Category 1 hurricane in 2002, was not included in the present study for lack of enough data to calculate the pre-hurricane VIs. To determine the study region of each hurricane, the VI change maps after a hurricane were first estimated (Eq. (3) in the Section 2.5). Then, the map showing the largest area of change on the path of hurricane was chosen. Finally, a region that contains densely distributed pixels with VI decrease higher than 10% was selected as the study region for a hurricane. To facilitate comparison, the same study region was applied in

Table 1
Characteristics of hurricanes that made landfall along the northern Gulf of Mexico from 2001 to 2015.

Name	Date	Wind speed (mph)*	Category*	Landing location
Ivan	2004.09.16	120	H3	Alabama
Charley	2004.08.13	150	H4	Florida
Frances	2004.09.05	105	H2	Florida
Jeanne	2004.09.26	120	H3	Florida
Katrina[δ]	2005.08.29	120	H3	Florida, Louisiana
Rita	2005.09.24	115	H3	Texas
Dennis	2005.07.10	120	H3	Florida
Wilma	2005.10.24	120	H3	Florida
Humberto	2007.09.13	90	H1	Texas
Gustav	2008.09.01	100	H2	Louisiana
Ike	2008.09.13	110	H2	Texas
Isaac	2012.08.29	80	H1	Louisiana

Note:
* It is the wind speed when a hurricane made landfall. The category was based on the Saffir-Simpson Hurricane Wind Scale.
δ Hurricane Katrina made its first landfall in Florida as category 1 hurricane on 2005.08.25.

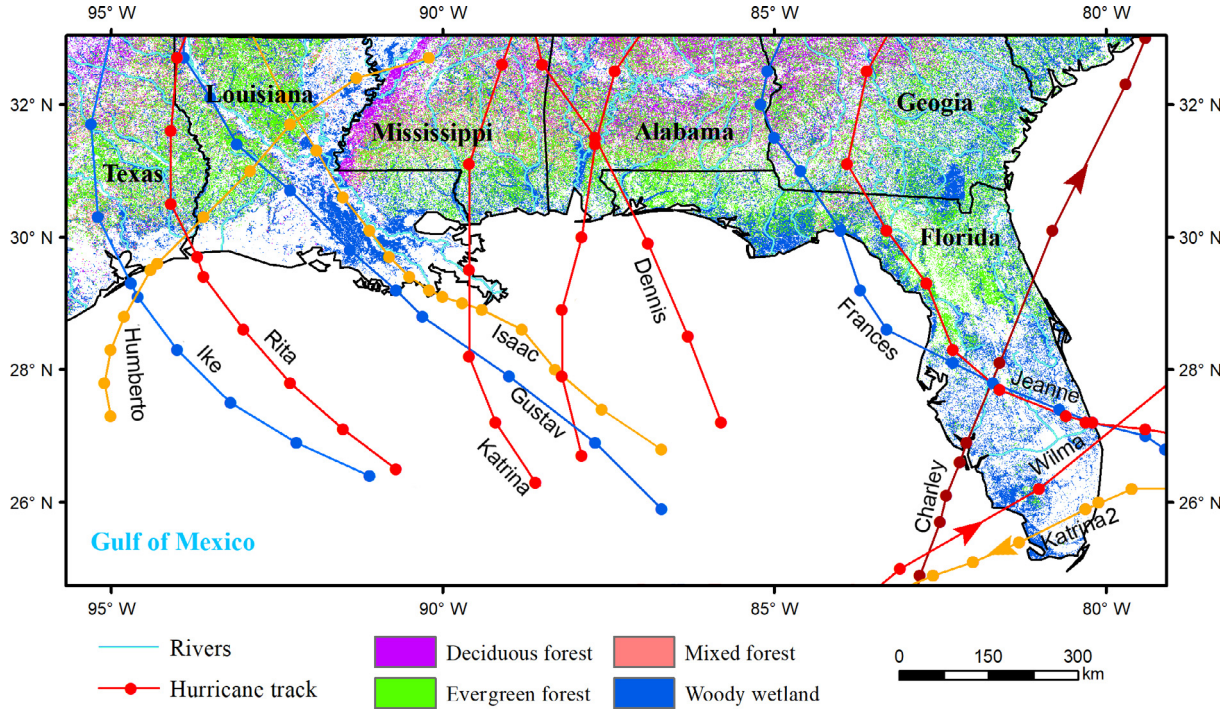

Fig. 1. Distribution of main forest types along northern Gulf of Mexico, and landfalls of hurricanes from 2001 to 2015. The dark red, red, blue, and brown colors indicate the tracks of Category 4, 3, 2, and 1 hurricane, respectively. (For interpretation of the references to colour in this figure legend, the reader is referred to the web version of this article.)

assessing VI changes during the pre-hurricane years and hurricane year for a specific hurricane. The study region of each hurricane event was shown in the supplementary files (Figs. S1–S5).

2.2. EVI, NDII, LAI, and SIF data

The EVI and NDII have been proved to be capable of detecting the forest damage induced by hurricanes (Wang et al., 2010; Wang and D'Sa, 2010). The MODIS bidirectional reflectance distribution function (BRDF) MCD43A4 version 6 dataset, with a 500 m spatial resolution, is produced daily using 16 days of Terra and Aqua data at Stage 3 validation. The view angle and atmospheric effects have been removed from this product, making it a more consistent and stable product than previous versions (Dahal et al., 2015; Schaaf and Wang, 2015; Wang et al., 2010). It is noted that the reflectance is often contaminated by smoke, high aerosol, or cloud around the days of disturbance (e.g. burning) or transient snow fall, which may increase the uncertainty of the MODIS BRDF products for those days (Wang et al. 2018). In the present study, the MCD43A4 dataset was used to derive the NDII and EVI from 2001 to 2015 along the Gulf coast.

LAI is a basic biophysical parameter that do not only control the biosphere–atmosphere exchanges of carbon and water, but also can capture the reflectance characteristics of vegetation in the canopy (Davi et al., 2008; Wang et al., 2010). The 8-day LAI data during 2001–2015 with a spatial resolution of 30 arc seconds (~1 km) was obtained from the Land-Atmosphere Interaction Research Group (http://globalchange.bnu.edu.cn/). This LAI dataset was reprocessed based on the MODIS LAI Collection 5 (C5) products. First, the low quality data was improved by using a modified temporal spatial filter method at the pixel level. Then, the post processing-TIMESAT (A software package for analysing time-series of satellite data) Savitzky-Golay filter was used to get the final result. As the improved LAI was established based on MODIS LAI dataset, its limitation mainly depends on the quality of MODIS LAI, which has a relatively low accuracy in equatorial regions (Yuan et al., 2011). Nonetheless, this version of LAI data has been proven to be closer to reference maps, and show a higher consistency in both time and spatial scales than the original MODIS LAI data (Jian et al., 2018; Wei et al., 2017; Yang et al., 2016; Yuan et al., 2011).

SIF can monitor rapid changes in the water stress of a canopy because it is directly related to the photosynthesis of vegetation (Wang et al., 2016). Therefore, it has been widely used in assessing environmental stress on ecosystems (Zarco-Tejada et al., 2009; Lee et al., 2013; Yoshida et al., 2015; Yang et al., 2018). The Global Orbiting Carbon Observatory-2 SIF (GOSIF) data covering the northern Gulf of Mexico during the 2001–2015 period was extracted from the dataset provided by the Global Ecology Group, University of New Hampshire (http://globalecology.unh.edu). This continuous dataset, with a high spatial and temporal resolutions (i.e., 0.05°, 8-day), was generated based on discrete OCO-2 SIF soundings, MODIS, and meteorological reanalysis data by using a data-driven approach (Li and Xiao, 2019). In addition to the potential uncertainty resulting from these gridded input data products, the omission of land cover types in predicting the SIF may also contribute to the uncertainty of this dataset (Qiu et al., 2020). Nonetheless, the GOSIF product has been proved to be able to capture seasonal cycles of vegetation, to monitor terrestrial photosynthesis, and to estimate the plant water stress (Li and Xiao, 2019; Xiao et al., 2019).

2.3. Forest cover data

The forest land cover data for the hurricane-impacted region along the northern Gulf of Mexico were retrieved from the National Land Cover Database 2011 product (https://www.mrlc.gov/data). Woody wetland was also included in this study as forested land with other three main forest types, namely deciduous forest, evergreen forest, and mixed forest (Fig. 1).

2.4. Drought data

The weekly drought condition data along the Gulf region during the 2001–2015 period was extracted from the United States Drought Monitor (USDM) (http://droughtmonitor.unl.edu). The USDM monitors the intensity and spatial extent of drought across the United States

(Svoboda et al., 2002). The drought maps are produced by weighing multiple drought indices according to their performance in various locations and times of the year. The other uniqueness of USDM dataset is the combination of judgement of climate and water experts, which makes it a more versatile result than other drought indices (Hao et al., 2017). Based on a percentile approach, the drought condition in USDM is grouped into four major categories, including moderate drought (D1), severe drought (D2), extreme drought (D3), and exceptional drought (D4). The fifth category D0 indicates abnormally dry conditions (Svoboda et al., 2002). The USDM dataset has been widely used in monitoring drought condition for scientific research and government plans. In the present study, the area percentage of D0, D1, D2, D3, and D4 from the total area of study region was used to reflect the drought condition for each study region per week.

2.5. Detection of hurricane damage

The short-wave infrared (SWIR) spectra is sensitive to liquid water absorption, whereas the near infrared (NIR) channel is insensitive to liquid water. The NDII was calculated based on the SWIR and NIR bands as follows (Eq. (1)):

$$NDII = \frac{(NIR - SWIR)}{(NIR + SWIR)} \quad (1)$$

where SWIR is the reflectance at 1.24, 1.65 or 2.13 mm wavelength. Previous studies have proved that the 2.13-mm band is superior due to the large amount of missing values at 1.65 mm channel caused by serious striping issue in the MODIS data (Dahal et al., 2015; Wang et al., 2010). NIR represents the 0.86 mm wavelength band.

The NIR, Red and Blue channels are used to calculate vegetation EVI (Eq. (2)):

$$EVI = G \times \frac{(NIR - \mathrm{Re}\,d)}{(NIR + C1 \times \mathrm{Re}\,d - C2 \times Blue + L)} \quad (2)$$

where NIR, Red, and Blue are the reflectance at 0.65, 0.86 and 0.47 mm wavelength for MODIS, respectively; C1 and C2 are coefficients of aerosol resistance term; L is a canopy background adjustment; and G is the gain factor. The coefficient values are C1 = 6, C2 = 7.5, L = 1, G = 2.5 (Huete et al., 2002; Wang et al., 2010).

ΔVI_{res}, which is defined as the ratio of a vegetation index (VI) reduction after and before the hurricane and the VI before the hurricane, was used to represent the forest resistance to hurricanes (Eq. (3)):

$$\Delta VI_{res} = \frac{(VI_{after} - VI_{before})}{VI_{before}} \quad (3)$$

where ΔVI_{res} means the VI changes when a hurricane made landfall; VI_{after} and VI_{before} refers to the observations at 16-day after and 16-day before a hurricane made landfall, respectively.

Forest resistance in the pre-hurricane years are calculated by using the Eq. (4):

$$\Delta VI_{prehu\_res} = \frac{(VI_{prehu\_after,i} - \bar{V}I_{prehu\_before,i})}{VI_{prehu\_before,i}},\ n \quad (4)$$

where ΔVI_{prehu_res} represents the multi-year averaged VI changes in pre-hurricane years; $VI_{prehu\_after,i}$ and $VI_{prehu\_before,i}$ refers to the VI value on the same day in a given pre-hurricane year i as VI_{after} and VI_{before} in the hurricane year, respectively, and n is the number of pre-hurricane years.

The net change of forest after a hurricane was computed as the difference between ΔVI_{res} and ΔVI_{prehu_res}, which is calculated as (Eq. (5)):

$$VI_{nc} = \Delta VI_{res} - \Delta VI_{prehu\_res} \quad (5)$$

2.6. Analysis of post-hurricane recovery

In this study, the post-hurricane recovery was specified to the ecological processes of the damaged forest canopy that caused by hurricanes to revert to the pre-hurricane status. This procedure was achieved by selecting an individual hurricane year and calculating the mean per-pixel VI for all 690 8-day periods of the 15-year time series extending from 2001 to 2015. VI anomalies were presented as departures of each of the 8-day periods from the 15-year averaged values (Eq. (6)). A cubic smoothing spline was fitted to the anomalies in order to better visualize interannual trends. VI anomalies during the entire 15-year period were created, but we focused on 4 years after major hurricanes and 2 years after Category 1 and 2 hurricanes. During the post-hurricane periods, when the value of the negative VI anomaly for a given 8-day period was higher than the averaged negative values at the pre-hurricane state, and this situation lasted at least for half a year, we deemed that the forest canopy have recovered from the hurricane. A similar approach was reported by Goetz et al. (2006) for detecting the post-fire recovery of forest across Canada.

$$VI_{anomaly} = VI_{i,j} - \bar{VI}_{i,15} \quad (6)$$

where $VI_{i,j}$ is the VI value of a pixel at a given 8-day period (i = 1, …, 46) of year j (j = 2001, 2002, …, 2015), $\bar{VI}_{i,15}$ is the temporal VI average for a specific 8-day period i over the 15 years of observation.

The detrended VIs, in which the seasonal signals were removed, were also created for evaluating the recovery process of forests after hurricane disturbances. The detrended VIs were calculated via “stl” using the “stats” package implemented in the R statistical software environment (RStudio Inc., Boston, MA, USA) (Cleveland et al., 1990). When the detrended post-hurricane VI was higher than that of the pre-hurricane status, the forest was considered to have recovered from the hurricane disturbance.

3. Results

3.1. Resistance and net change of forest VIs after hurricanes

Post-hurricane forest damage was detected by evaluating the resistance and net change based on the four VIs. The three Category 3 hurricanes, namely Ivan, Katrina, and Rita, caused NDII decreases ($NDII_{res}$) of 17.39%, 15.15%, and 16.07%, respectively, which led to net NDII decreases ($NDII_{nc}$) of 11.97%, 12.38%, and 12.39% compared to the NDII in the previous years without hurricane disturbances, respectively (Fig. 2A). In contrast, the NDII increased slightly (0.57%) after the landfall of Hurricane Dennis. This amount of increase was 1.61% lower than that of the pre-hurricane state. A positive NDII resistance of 3.58% was also found in the impact region of Hurricane Charley, which led to a 0.69% of net NDII decrease. Hurricanes Frances and Jeanne caused immediate NDII decrease of 2.19% and 5.35%, and 1.66% and 0.47% of net decreases, respectively. In contrast, Katrina2 and Wilma caused higher immediate NDII decrease of 2.67% and 9.61%, respectively.

After Hurricane Humberto, the NDII decreased by 4.94% in the impact region but was 3.90% higher than the NDII in the previous years without hurricane disturbances (Fig. 2A). This indicated that Hurricane Humberto did not cause an additional decrease of NDII in this region, but contributed to the increasing trend of the NDII to some extent. In contrast, the NDII decreased by 14.08% after Hurricane Gustav struck this region in 2008, which was 7.61% lower than the NDII in previous years without hurricane disturbances. The landfall of hurricanes Ike and Isaac led to the immediate reductions of NDII by 14.56% and 15.12%, respectively, corresponding to 10.68% and 7.21% of net decreases compared to the conditions without hurricane disturbances (Fig. 2A).

The positive net VI change after Hurricane Humberto was also

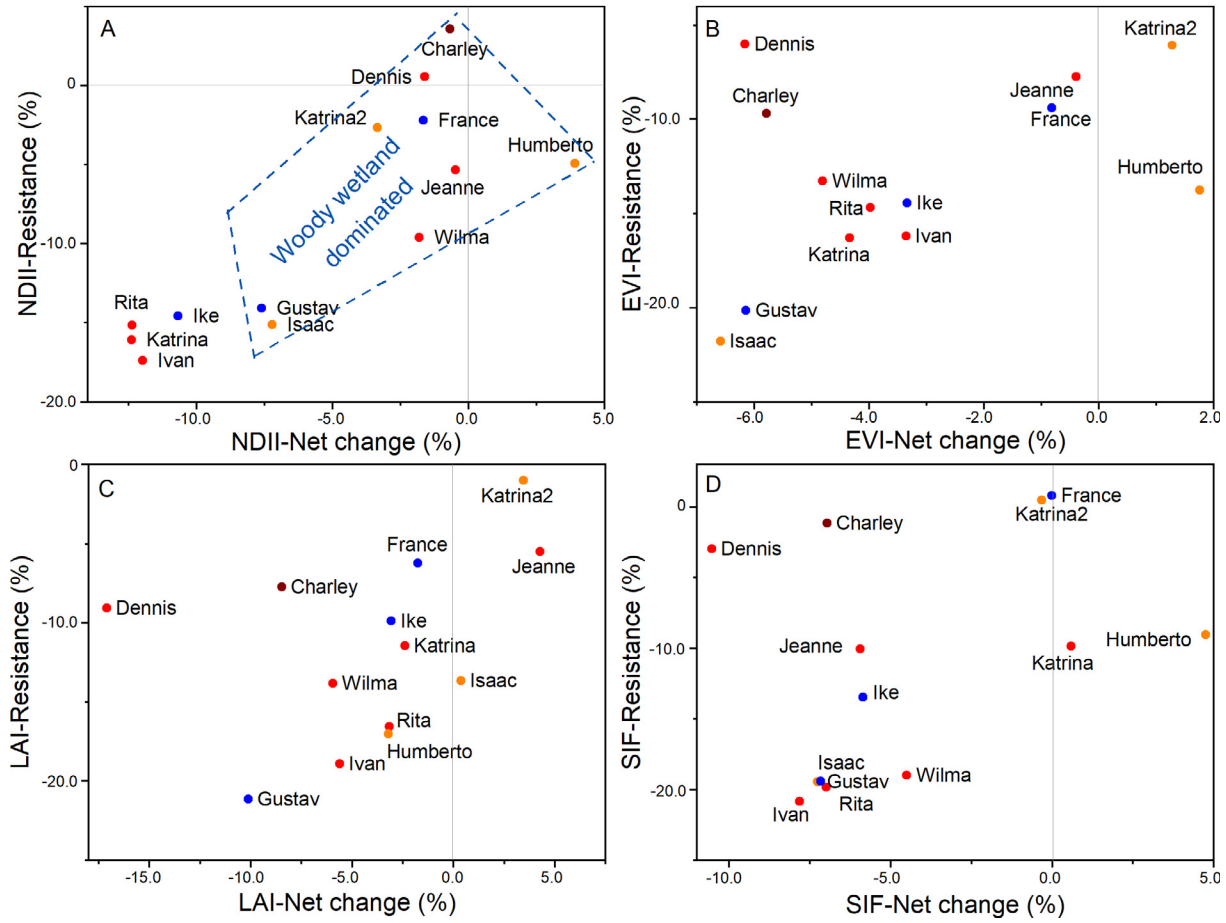

Fig. 2. Comparison of forest resistance and net change of VIs induced by hurricanes from 2001 to 2015. The dark red, red, blue, and brown colors indicate the Category 4, 3, 2, and 1 hurricane, respectively. (For interpretation of the references to colour in this figure legend, the reader is referred to the web version of this article.)

observed in the EVI and SIF values (Fig. 2B and D). Forests in Florida displayed higher resistance to hurricanes than that of forests on the northern Gulf coast, even after major hurricanes (Charley, Jeanne, and Wilma). This pattern was reflected in all the four VIs, with an approximate 10% of decrease in each (Fig. 2). The EVI presented a level of resistance similar to that of the NDII after hurricanes Ivan, Katrina, and Rita. The NDII change also clearly displayed a lower net change in woody wetland-dominated forests than in evergreen forest-dominated regions (Gustav vs. Ike, Jeanne/Wilma vs. Rita/Katrina/Ivan). The EVI results revealed that the forests impacted by Hurricane Gustav (category 2) and Hurricane Isaac (category 1) exhibited lower resistance and net change than the levels associated with any other hurricanes (Fig. 2).

3.2. Seasonal and interannual dynamics of post-hurricane VIs

The seasonal and interannual dynamics of the pre- and post-hurricane VIs were evaluated in order to reflect the impacts of hurricanes on forests. In 2004, the landfall of Hurricane Ivan caused a sudden drop in the NDII (Fig. 3A). The NDII values over the following month were noticeably lower than those of the pre-hurricane period but then rebounded and eventually approached the pre-hurricane values. The NDII values in the winter and spring of 2005 were clearly lower than those of previous years, however. The impact of Hurricane Dennis in the early summer of 2005 caused a weak decrease of NDII in the same region. A drought occurred and intensified from the mid-spring to the late summer of 2006, which aggravated the decrease of NDII during this period. However, even though a relatively weak drought extended from the spring to the early autumn of 2007, the NDII increased gradually over that period. A similar seasonal pattern was also found in the EVI and SIF trends. In contrast, the lowest value of the LAI was observed in the summer of 2005. The annual change trends of NDII, EVI, and SIF all exhibited the largest decreases in 2006 and increased gradually thereafter.

The landfall of Hurricane Katrina brought more severe damage to the impact area, resulting in NDII values during the following 3 months were markedly lower than those of the years without hurricanes (represented by the black dotted line in Fig. 3B). The intensified drought from mid-spring to late-summer caused an apparent decrease of NDII values relative to those of previous years without hurricanes. Compared with the averaged value in the respective seasons from 2001 to 2004, the mean NDII decreased by 0.029, 0.049, 0.054, and 0.052 in the winter, spring, summer, and autumn of 2006, respectively. By the first half year of 2009, the NDII values were close to their pre-hurricane levels. The EVI and SIF dynamics also captured these trends but with smaller change magnitudes. In contrast, these trends were not detected by the LAI. The annual NDII, EVI, and SIF experienced their maximum decreases in 2006, after which they began to increase.

The sudden decrease of the NDII was also observed when Hurricane Rita made a landfall and continued for the following 40 days (Fig. 3C). In contrast, the EVI, LAI, and SIF did not exhibit clear reductions after Hurricane Rita, and annual values that were even higher than pre-hurricane conditions were observed in these three VIs. Despite hurricanes Charley, Frances, and Jeanne making landfalls in 2004, the VIs in the study region did not suddenly decrease (Fig. 3D). After hurricanes Katrina and Wilma made landfall in 2005, the NDII still did not decrease immediately. It was in 2006 that the NDII decreased

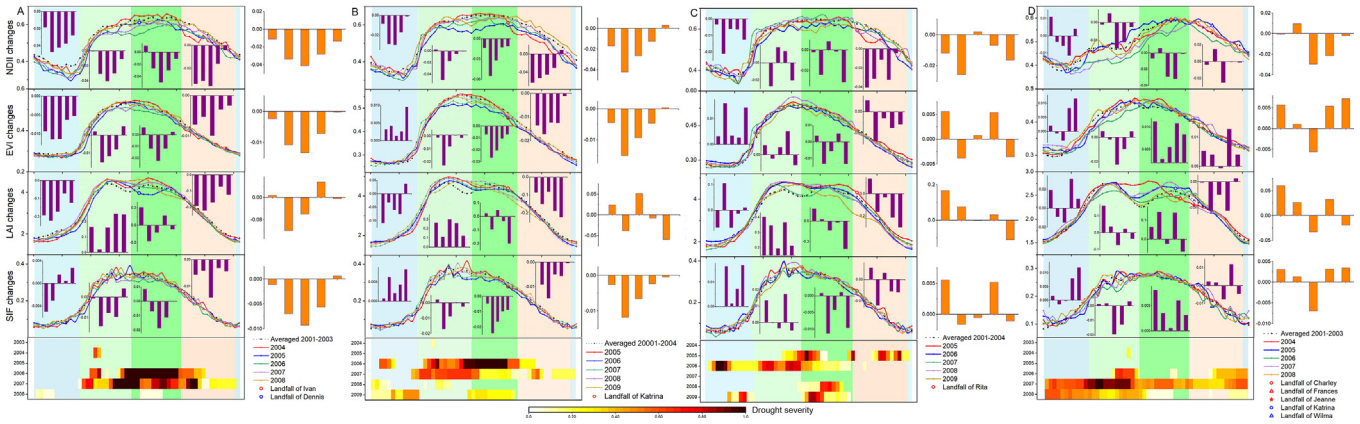

Fig. 3. Seasonal and interannual VI trends, and the drought condition over the same period in the impacted region after hurricanes (A) Ivan-Dennis, (B) Katrina, (C) Rita, and (D) Charley-Frances-Jeanne-Katrina-Wilma. The drought severity is represented by the percentage of the total area of D1, D2, D3, and D4 to the area of the entire study region. The light blue, light green, green, and light orange background colors of each panel indicate winter (Dec. 22 (former year) to Mar. 20), spring (Mar. 21 to Jun. 21), summer (Jun. 22 to Sept. 22), and autumn (Sept. 23 to Dec. 21), respectively. The purple histograms represent the seasonal anomalies of VIs compared with seasons in years without hurricane disturbances. The orange histograms denote the annual anomalies of VIs compared with years without hurricane disturbances.

significantly, particularly in the spring and summer. The widespread drought during the entire year of 2007 hindered the increase of the NDII. Even so, NDII was close to the pre-hurricane level by the autumn of 2007. In contrast, the values of EVI, LAI, and SIF in 2007 were well above the average values without hurricanes disturbances.

For Category 1 and 2 hurricanes, the sudden decrease of VIs, with the exception of the LAI, was detected when hurricanes Gustav, Ike, and Isaac each made landfall (Fig. 4A–C). The landfall of Hurricane Humberto caused very small of VI decreases. Despite the impact of Hurricane Gustav, the annual NDII was still higher than the value in years without hurricane disturbances. In contrast, the EVI, LAI, and SIF values were lower than pre-hurricane levels. The landfall of Hurricane Ike brought a longer period of damage to the impacted region. NDII values lower than those of the pre-hurricane period lasted for nearly three months after its landfall. The largest decrease of VIs occurred in 2009. The drought condition in the summer of 2009 may have also contributed to the decrease. By the autumn of 2009, the NDII, EVI, and SIF values were all close to their pre-hurricane levels.

3.3. Analysis of the post-hurricane forest recovery

The response of VI anomalies to hurricanes over time is depicted in Figs. 5 and 6. For major hurricanes, the VI anomalies drastically dropped when the hurricanes made landfall (Fig. 5). The NDII anomaly reached its minimum value of −0.068 24 days after Hurricane Ivan struck the Gulf region, which was nearly 20 times lower than the variation in 2003 (Fig. 5A). The NDII anomaly then increased gradually, but dropped again at the beginning of 2005, reaching its minimum at the end of winter, and increasing in the spring. In the early summer of 2005, Hurricane Dennis made a landfall as a Category 3 hurricane in this region, which caused a sudden decrease of the NDII. However, the amount of decrease was lower than that caused by Ivan. The NDII

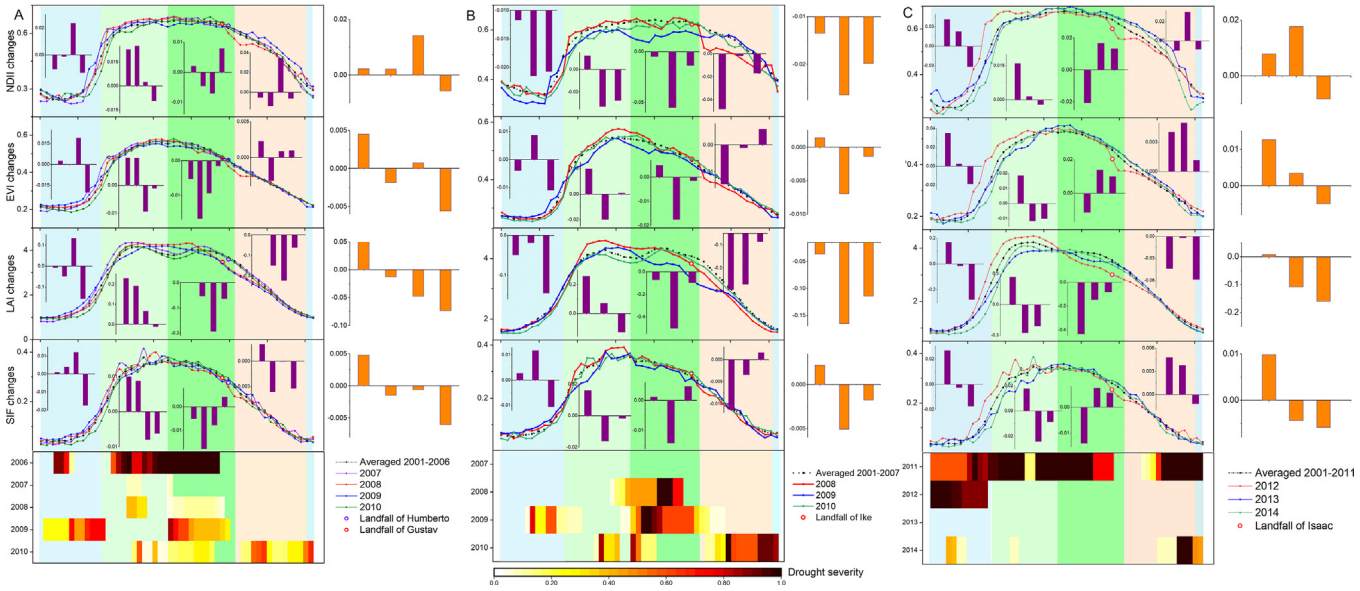

Fig. 4. Seasonal and interannual VI trends, and the drought condition over the same period in the impacted region after hurricanes (A) Humberto-Gustav, (B) Ike, and (C) Isaac. The drought severity is represented by the percentage of the total area of D1, D2, D3, and D4 to the area of the entire study region. The light blue, light green, green, and light orange background colors of each panel indicate winter (Dec. 22 (former year) to Mar. 20), spring (Mar. 21 to Jun. 21), summer (Jun. 22 to Sept. 22), and autumn (Sept. 23 to Dec. 21), respectively. The purple histograms represent the seasonal anomalies of VIs compared with seasons in years without hurricane disturbances. The orange histograms denote the annual anomalies of VIs compared with years without hurricane disturbances.

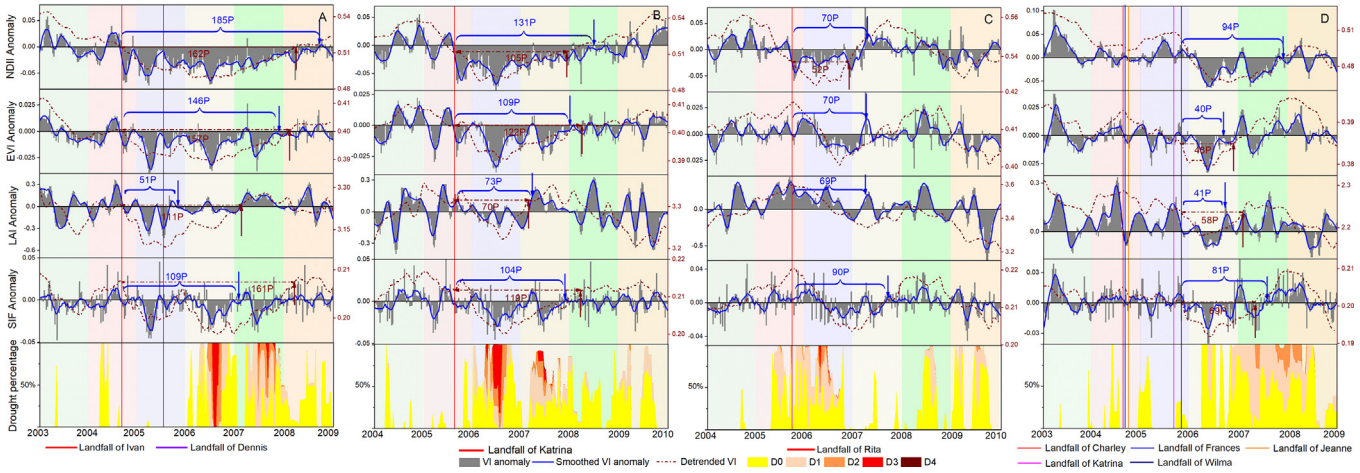

Fig. 5. Variations of VI anomalies and detrended VIs, and the drought condition over the same period in the impacted region after hurricanes (A) Ivan-Dennis, (B) Katrina, (C) Rita, and (D) Charley-Frances-Jeanne-Katrina-Wilma.

increased 40 days after Dennis struck. Simultaneously, a drought expanded and intensified aggressively in this region, beginning in the late spring and lasting until the early autumn. The widespread drought exacerbated the reduced NDII anomaly, which reached a minimum value of −0.071. As the drought abated, the NDII anomaly increased steadily, despite the drought conditions in 2007. The forest NDII had recovered by the early autumn of 2008, which was approximately 4 years after the landfall of Hurricane Ivan (185P, where 1P = 8 days). The detrend NDII had been declining since 2003 and reached the minimum in the autumn of 2006 when the extreme drought occurred. The detrended NDII recovered to its pre-hurricane level by the beginning of 2008, which was nearly 6 months earlier than that monitored by the NDII anomaly (162P). The EVI anomaly exhibited a pattern similar to that of the NDII, albeit with a more pronounced variation. The reduced magnitude of the EVI anomaly caused by Hurricane Dennis was comparable to that resulting from Hurricane Ivan. The second-largest decrease of the EVI anomaly occurred during the extreme drought in 2006, and the third-largest decrease corresponding to the widespread drought in 2007. The SIF anomaly shared a pattern similar to that of the EVI. The LAI anomaly recovered to pre-hurricane levels by the autumn of 2005, which was less than 4 months after the landfall of Hurricane Dennis, implying that the forest LAI was less responsive to hurricanes.

The recovery trajectories after Hurricane Katrina displayed a pattern similar to the recovery after Hurricane Ivan. The NDII anomaly indicated that the recovery process began approximately 50 days after Hurricane Katrina made landfall (Fig. 5B). The extreme drought in 2006 led to the largest decrease of the NDII, EVI, and SIF anomalies. The drought conditions in 2007 also contributed to the decreases of EVI and SIF. In general, the NDII, EVI, and SIF anomalies all demonstrated that the forest canopy had returned to pre-Katrina conditions by the end of 2007 or the first half year of 2008 (NDII: 131P; EVI: 109P; SIF: 104P), whereas the LAI anomaly exhibited a faster recovery, as it had rebounded by the winter of 2007 (73P).

A shorter recovery process was recorded in Hurricane Rita impacted region. The NDII anomaly indicated that the forest began to recover less than a month after Rita hit, and had recovered to pre-hurricane conditions by the early spring of 2007 (70P) (Fig. 5C). In contrast, the EVI and SIF anomalies decreases slightly after Hurricane Rita made landfall,

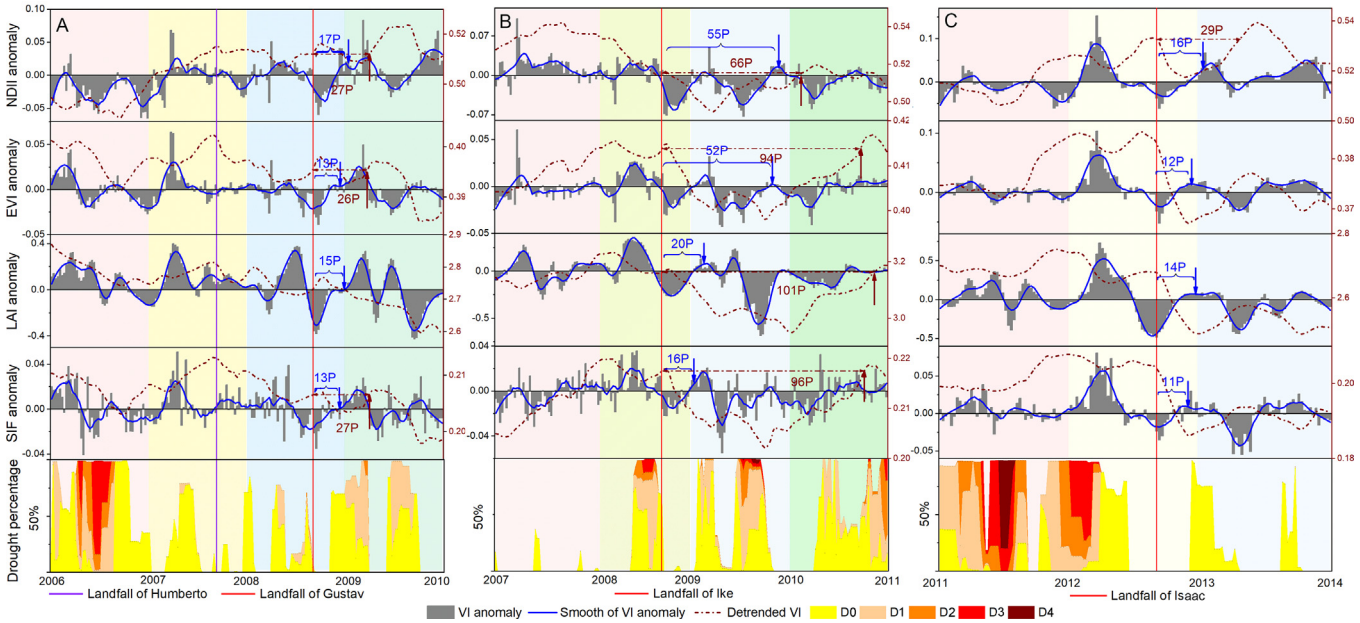

Fig. 6. Variations of VI anomalies and detrended VIs, and the drought condition over the same period in the impacted region after hurricanes (A) Humberto-Gustav, (B) Ike, and (C) Isaac.

and were even higher than their pre-hurricane values approximately one month later, maintaining those levels to the end of winter of 2006. The LAI anomaly was higher than the average level despite the impact of Hurricane Rita. The detrended EVI, LAI, and SIF variations failed to monitor the forest recovery to the pre-hurricane levels.

The VI anomalies decreased slightly after hurricaness Charley, Frances, and Jeanne made landfall in 2004, which were comparable to the fluctuations without hurricane disturbances in the study region (Fig. 5D). In 2005, hurricanes Katrina and Wilma made landfall in southern Florida, which has relatively high forest coverage compared to the middle and north of study area. Since the decreasing trend of VI anomalies was mainly concentrated in this region, the recovery period was calculated after the landfalls of hurricanes Wilma and Katrina. The largest decrease of VI anomalies occurred in the spring of 2006, while the following noticeable decrease took place in the spring of 2007, when a moderate drought expanded concurrently in this region. The NDII anomalies exhibited recovery periods longer than those simulated by the EVI, LAI, and SIF anomalies (NDII: 94P; EVI: 40P; LAI: 41P; SIF: 81P).

The landfall of Hurricane Humberto in 2007 caused slight disturbance to the VI anomalies. In contrast, VI anomalies decreased markedly after the impact of Hurricane Gustav (Fig. 6A). Generally, the VI anomalies began to increase less than a month after a hurricane, and recovered to pre-disturbance conditions within approximately 5 months (NDII: 17P; EVI: 13P; LAI: 15P; SIF: 13P). The variations of VI anomalies after the landfall of Hurricane Isaac exhibited a similar pattern (NDII: 16P; EVI: 12P; LAI: 14P; SIF: 11P) (Fig. 6C). In the region impacted by Hurricane Ike, the NDII and EVI anomalies displayed a recovery period lasting nearly 15 months (NDII: 55P; EVI: 52P), which was longer than the time periods based on the LAI and SIF anomalies (LAI: 20P; SIF: 16P) (Fig. 6B). The detrend VI variations displayed longer recovery periods than the variations of VI anomalies in the regions impacted by hurricanes Gustav, Ike, and Isaac.

4. Discussion

4.1. Factors that affect forest resilience to hurricanes

Hurricane impacts are largely determined by wind speed, forest structure, environmental conditions and the topography of a given area (Stanturf et al., 2007; Chapman et al., 2008). Wind speed is the most influential factor affecting the severity of forest damage. Category 1 and 2 hurricanes, with sustained wind speeds of 74–110 mph, will cause large tree branches to snap and trees with shallow roots to topple, while major hurricanes with sustained wind speed ≥111 mph will result in the snapping and uprooting of most trees (Schott et al., 2019). Our results revealed that for the hurricane-impacted regions dominated by evergreen forests, the net change of the NDII decreased by 12.37%, 12.38%, and 11.97% after hurricanes Rita, Katrina, and Ivan (all three are major hurricanes), respectively. After Hurricane Ike (Category 2), the net change of the NDII decreased by 10.68%. For the woody wetland-dominated region, a slightly higher decrease of net change of the NDII was observed after Hurricane Gustav (Category 2) than that after Hurricane Isaac (Category 1). Previous studies have also revealed that the EVI decreased more after hurricanes Katrina and Rita than that after hurricanes Gustav, Ike, and Lily (Wang and D'Sa, 2010). It is worth noting that despite being impacted by Dennis (a major hurricane) in 2005, the affected region exhibited a 1.61% net decrease of the NDII and positive resistance. This small net decrease was probably due to the fact that most susceptible trees had already died in this region as a result of Hurricane Ivan, and the impacted trees were still undergoing recovery. The positive resistance can partially be explained by the fact that Dennis made landfall in early summer, when the NDII of forests is increasing. At the stand scale, the underlying topographic or geomorphic features would influence the secondary wind speed and wind direction, especially where local topography is complex (Boose et al., 1994, 2004; Wang and Xu, 2009). The wind speed would be accelerated over ridges and summits with strong turbulence on the steep slopes. In the hilly or mountainous regions, the local topography may modify the wind direction as the winds are channeled along alternative routes (Boose et al., 1994). In contrast, no significant impact of topography on forest damage was observed in the two riparian zones after the Hurricane Georges (Zimmerman and Covich, 2007).

Forest type is another factor affecting the forest resilience to hurricanes. For regions affected by Category 3 hurricanes, the areas dominated by evergreen forests that were impacted by hurricanes Rita, Katrina, and Ivan all showed similar resistance levels and net NDII changes, which were higher than those of regions dominated by woody wetlands that were affected by hurricanes Wilma and Jeanne (Fig. 2A). Likewise, the regions dominated by evergreen forests that were hit by Hurricane Ike presented a larger net NDII change (−10.68%) than the regions dominated by woody wetlands that were hit by Hurricane Gustav (−7.61%) (Fig. 2A), although the opposite phenomenon was observed in the EVI and SIF changes. Previous studies have shown that even though the wetland forests experience very high wind speeds, their damage is largely limited to foliage loss (Frangi and Lugo, 1991; Ramsey et al., 2009; Tanner et al., 1991). The bald cypress trees in flooded areas exhibit strong structural stability against bole and branch snap because of the unique root system resistant to wind damage (Chapman et al., 2008; Wang and Xu, 2009). Soil physical and chemical properties that contribute to the development of deep root system would benefit a higher resistance to wind damage (Wang and Xu, 2009). Other studies, however, have argued that wetland forests are less resistant to hurricanes than rain forests and semi-deciduous dry forests with high biodiversity (Imbert et al., 1998, 2018). Since the ground observation results are highly dependent on the choice of tree species, long-term monitoring data are still required to clarify this question. Nonetheless, the NDII, EVI, and SIF anomalies all indicated that longer recover time was needed for the region impacted by Hurricane Ike than the region impacted by Hurricane Gustav, implying that evergreen forests are more vulnerable than woody wetlands when experiencing the same category of hurricane. Even for woody wetlands, the regions impacted by hurricanes Gustav and Isaac exhibited higher values of net NDII change than the values after hurricanes Charley, Frances, Jeanne, and Wilma. This is probably due to the low areal coverage of woody forests in the Florida study region. Larger uncertainty may exist in the assessment of forest damage in these regions. In addition, the heavy rain brought by hurricanes stimulates the fast growth of forests in the upland regions, which offsets the decrease of VIs caused by hurricanes (Wang and D'Sa, 2010). The recovery of the forest canopy gap mainly depends on the combination of branch resprouting and the growth of germinated seedlings/saplings (Burslem et al., 2000; Tanner et al., 1991). Some studies have pointed out that a replenishment strategy of new or pre-established seedlings dominates the recovery of mangrove forests (Baldwin et al., 2001; Imbert, 2018).

We also discovered that drought conditions during the post-hurricane period also affect the forest recovery trajectory. Our simulation revealed that after a major hurricanes struck an area, the decreasing trends of NDII, EVI, and SIF persisted in the following year. This is due to the delayed dieback and mortality of disturbed vegetation, which lead to additional losses in the impacted forests (Chapman et al., 2008; Wang and D'Sa, 2010). Regions impacted by hurricanes Katrina and Ivan-Dennis experienced extreme drought in the summer of 2006, which led to larger decreases of the NDII and EVI than when the hurricanes made landfall. Despite the rapid releafing and resprouting of the most damaged stems, drought may aggravate the continuous tree mortality or slow down the weak photosynthetic capacity of a few new shoots. A longer recovery period has been observed in a lake ecosystem after a hurricane following a major drought (Xuan and Chang, 2014). For the regions dominated by evergreen forests that were impacted by major hurricanes, a longer recovery period was observed in the area affected by Hurricane Katrina impacted region (NDII: 131P) than the

region affected by Hurricane Rita (NDII: 70P) where experienced a subsequent moderate drought. The concurrence of drought and noticeable decrease of the NDII was also observed in the region impacted by Hurricane Ike. de Beurs et al. (2019) discovered that a MODIS-based disturbance index is capable of detecting the impact of droughts and hurricanes on the four largest Caribbean islands. It remains challenging, however, to determine how long a subsequent drought can delay the post-hurricane recovery, since recovery length is affected by not only the duration and intensity of drought but also the characteristics of hurricanes and forest types.

Post-hurricane recovery was also found to be associated with the hurricane frequency. Regions dominated by evergreen forests generally require more than one growing season to recover from a major hurricane. The landfall of a subsequent hurricane extends the recovery period to some extent. In our study, the NDII anomaly revealed that it took 185P for the impacted forest to recover from hurricanes Ivan and Dennis, whereas forests with similar habitats needed 131P to get recovered from Hurricane Katrina. The EVI anomaly also indicated that the recovery period from hurricanes Ivan-Dennis was nearly 10 months longer than from Hurricane Katrina. The landfall of Hurricane Dennis re-destroyed the vegetation that was recovering from Hurricane Ivan. The continuous intrusion of saline water causes salt contamination to coastal vegetation and inflicts long-term damage on marshes, which affects forest recruitment more than the uprooting and/or snapping of trees (Brun and Barros, 2013; Wang and D'Sa, 2010). The cases of hurricanes Humberto-Gustav and Isaac demonstrated that woody wetlands can recover from Category 1 and 2 hurricanes within one growing season before the next hurricane season.

4.2. Uncertainty and future research

The detection of forest damage relies heavily upon the selection of vegetation indicators. The NDVI and EVI are the most commonly used indicators for identifying the forest damage induced by disturbances (Ramsey et al., 2001; Ayala-Silva and Twumasi, 2004; Goetz et al., 2006; Rogan et al., 2011; Yang et al., 2017). In this study, we selected EVI over the NDVI due to the saturation of the NDVI over the dense canopy in tropical and sub-tropical regions (Rogan et al., 2011; Wang et al., 2010). SIF was included in our investigation to detect the forest resilience to hurricanes given its sensitivity to changes in canopy structure and pigment concentration. SIF has been widely used in monitoring drought restrictions on vegetation photosynthesis (Zhang et al., 2019; Wang et al., 2016; Yang et al., 2018). Our results revealed that SIF demonstrated a performance similar to that of the EVI in identifying the forest damage and monitoring the post-hurricane recovery process. Due to the coarse spatial resolution of currently available time series data, however, the SIF variations exhibited more disperse distribution than those of the EVI. Since the NDII is calculated based on the NIR and SWIR bands, it can reflect the leaf water content after disturbances. The NDII has proven to be superior in detecting the forest damage after hurricanes (Dahal et al., 2015; Wang et al., 2010). This study also found that the sensitivity of NDII to hurricane disturbances was greater than the EVI, LAI, and SIF in terms of detecting the forest resistance and net change after hurricanes. The NDII also outperformed the other VIs in monitoring the recovery process of the forest canopy, particularly for the regions impacted by Hurricane Rita.

The defoliation caused by strong winds leads directly to the contraction of the forest canopy, and the LAI was thus expected to decrease markedly. A sudden decrease of LAI was not observed after hurricanes Dennis, Katrina, Jeanne, and Isaac, however, and even though decreasing LAI trends were observed after hurricanes Rita and Humberto, the LAI values were still higher than the 15-year averaged values. Despite different data sources, the inferior performance of the LAI was also identified when detecting the forest damage caused by Hurricane Katrina (Wang et al., 2010). One reason for this may be that the broken or fallen branches with leaves can still survive for a certain period, implying that the leaf area would not decrease immediately. Moreover, the rapid resprouting of damaged trees and the vigorous growth of understory vegetation after hurricanes compensate for the decrease of LAI.

In addition to the VI selection, the forest damage map is also affected by the comparison dates representing the pre- and post-hurricane states. The dense cloud cover brought by hurricanes always causes a great deal of missing remote sensing data, particularly in the coastal areas, where 80% of the data are contaminated by cloud (de Beurs et al., 2019). Therefore, it is difficult to select the standard "before and after" comparison dates when identifying an impact region. In this study, the averaged 8-day NDII and EVI were calculated based on daily values. We used the date of 16 days prior to hurricane landfall as the pre-hurricane date, and 16 days after landfall as the post-hurricane date. The image difference between 16 days before and after hurricanes has been used in previous studies to detect hurricane impacts (Wang et al., 2010; Wang and D'Sa, 2010). Wang and D'Sa (2010) concluded that the EVI value at one month after a hurricane and the image difference between one year just prior the hurricane and the year with the hurricane was optimal in reflecting the hurricane-induced damage. However, based on our results, the timing for comparison cannot be extended to months because forests can recover quickly after hurricanes, particularly after Category 1 and 2 hurricanes, which can explain why the disturbance pattern could not be detected by using the two EVI images between the years after hurricanes Gustav and Lili in their study.

Uncertainty also exists in the method that used to assess the recovery period of impacted forests. Generally, there are two methods used to investigate the recovery of forests after disturbances, which are referred to as "comparison with pre-disturbance conditions" and "comparison with undisturbed regions" (Yang et al., 2017). In this study, the return to the pre-hurricane state of the canopy cover (the "comparison with pre-hurricane status" method) was employed, which was achieved by comparing the post-hurricane VI values with those of the pre-hurricane period. This approach has been used in assessing the forest recovery after fire disturbances (Goetz et al., 2006; Yang et al., 2017). The "comparison with undisturbed regions" method was not adopted in this study due to the large regions that were impacted by the hurricanes. Moreover, most of the regions in the coastal area were frequently disturbed by the hurricanes. Therefore, it was difficult to locate an "undisturbed region" with similar environmental conditions and topography as the entire hurricane-impacted region. One of the primary challenges when detecting the long-term VI changes is to eliminate the effects of vegetation phenology. $VI_{anomaly}$ was therefore calculated for the same 8-day calendar period from 2001 to 2015, which allowed the detection of VI changes without the impacts of seasonal signals and the determination of the disturbance attributes (Goetz et al., 2006; Brun and Barros, 2013). In this study, the disturbance history of the trees in each study region, such as logging, insect or diseases outbreaks, and fires, was not taken into consideration due to the lack of observation data, which may lead to uncertainties. The different effects of climate variations, CO_2 fertilization, and nitrogen deposition during the pre- and post- hurricane periods would also cause uncertainties. The detrended VI variations can monitor the recovery of the forest canopy to some extent. However, they fails to return to pre-hurricane levels, probably due to the decaying trend of VIs, such as the detrended EVI, LAI, and SIF after hurricanes Rita and Isaac.

The selection of the study region may be another source of uncertainty. In this study, the forest resilience was evaluated based on the averaged VI of the study region after hurricanes. The study regions, however, do not represent the entire region that is impacted by hurricanes (Figs. S1–S5). For example, the study regions for hurricanes Katrina and Rita mainly incorporated the severe and moderate damage regions estimated by the Forest Inventory and Analysis, USDA Forest Service (Negrón-Juárez et al., 2010; Ramsey et al., 2009; Wang et al.,

2010; Clark et al., 2006). In the study by Wang et al. (2010), a major impacted region was selected to derive the statistical variables, and they found that the net changes of the NDII and EVI decreased by 17% and 4%, respectively, after Hurricane Katrina compared with the same period in 2003. Meanwhile, our estimation (which utilized a larger study region) showed that the decreases of the NDII and EVI net change were 12.4% and 4.3%, respectively. The heavy rain associated with hurricanes promotes the rapid growth of vegetation, particularly in upland forests, thus leading to the underestimation of damage after a disturbance if a larger region is considered.

This study provides comprehensive insight into the forest resilience to hurricanes. Future research could potentially be improved in the following way. Multi- and hyperspectral remote sensing images with higher spatial resolution could be collected in order to provide more accurate estimations of forest dynamics after hurricane disturbances. Based on these images, a forest damage map could be retrieved with appropriate upscaling strategies at a large scale. State-of-the-art technology, such as artificial intelligence, could then be utilized to generate time-series forest maps at pre- and post- hurricane states. These maps could be employed as inputs to force the Earth System models to evaluate the impacts of hurricane disturbances on the carbon, nitrogen, and water cycles of forest ecosystems. From the Earth System modeling perspective, the consideration of vegetation-specific post-hurricane regeneration strategies (such as resprouting and seedling/sapling growth), vegetation succession, and forest age structures will help to improve the simulation of post-hurricane recovery. Moreover, the high-resolution images and ground observations would be beneficial to the parameterization scheme of the models and the prediction of future damage.

5. Conclusions

In this study, we used four remotely-sensed VI indicators, namely NDII, EVI, LAI, and SIF, to evaluate the forest resilience to hurricanes along the northern Gulf of Mexico from 2001 to 2015. Wind speed, i.e. hurricane intensity, is the leading factor affecting forest resilience. Generally, the impacted forest canopy began to recover approximately one month after the hurricane landfall. The impacts of hurricanes were found to be stronger in regions dominated by evergreen forests than in regions dominated by woody wetlands. The seasonal dynamics of the NDII indicated that after the impact of major hurricanes, NDII values lower than the multi-year averaged values were observed across all seasons in the following year even without drought, implying that previous research may have underestimated the forest carbon loss induced by major hurricanes when only the damage in the hurricane year was taken into consideration. We discovered that the drought conditions during the post-hurricane period also affect the forest recovery. It should be noted that the satellite observations of forest canopies may indicate a quick reversion to pre-hurricane conditions, whereas the structural recovery of vegetation will likely take decades to return to pre-hurricane levels. The integration of multiple sources of ground and satellite data with Earth System models will facilitate a better understanding of the response of forest ecosystems to hurricanes.

CRediT authorship contribution statement

Chengcheng Gang: Conceptualization, Methodology, Writing - original draft, Funding acquisition. **Shufen Pan:** Conceptualization, Resources, Writing - review & editing. **Hanqin Tian:** Conceptualization, Resources, Supervision, Funding acquisition. **Zhuonan Wang:** Data curation, Investigation. **Rongting Xu:** Validation, Writing - review & editing. **Zihao Bian:** Data curation, Visualization, Investigation. **Naiqing Pan:** Data curation, Visualization. **Yuanzhi Yao:** Data curation, Writing - review & editing. **Hao Shi:** Software, Validation.

Acknowledgment

This work was supported by the National Natural Science Foundation of China, China (31602004); the National Key Research and Development Program of China, China (2016YFC0501707); the CAS "Light of West China" program, China (XAB2016B05); the Fundamental Research Funds for the Central Universities, China (2452017184); NSF-NSFC Joint INFEWS Project (1903722), China and United States; NOAA Center for Sponsored Coastal Ocean Research (NA16NOS4780204), United States, and OUC-AU Joint Center Research Program, China and United States. We also appreciate the China Scholarship Council for the financial support, and the Land Processes Distributed Active Archive Center, the Land-Atmosphere Interaction Research Group at Sun Yat-sen University, the Global Ecology Group at University of New Hampshire, U.S. Drought Monitor, and Multi-Resolution Land Characteristics (MRLC) Consortium for sharing dataset.

Appendix A. Supplementary material

Supplementary data to this article can be found online at https://doi.org/10.1016/j.foreco.2020.118243.

References

Aosier, B., Kaneko, M., Takada, M., 2007, Evaluation of the forest damage by typhoon using remote sensing technique. In: IEEE International Conference on Geoscience and Remote Sensing Symposium, IGARSS, Barcelona, Spain, pp. 3022–3026.
Ayala-Silva, T., Twumasi, Y.A., 2004. Hurricane Georges and vegetation change in Puerto Rico using AVHRR satellite data. Int. J. Remote Sens. 25, 1629–1640.
Baldwin, A., Egnotovich, M., Ford, M., Platt, W., 2001. Regeneration in fringe mangrove forests damaged by Hurricane Andrew. Plant Ecol. 157, 151–164.
Bellingham, P.J., Tanner, E., Healey, J.R., 1995. Damage and responsiveness of Jamaican montane tree species after disturbance by a hurricane. Ecology 76, 2562–2580.
Beven, J.L., Avila, L.A., Blake, E.S., Brown, D.P., Franklin, J.L., Knabb, R.D., Pasch, R.J., Rhome, J.R., Stewart, S.R., 2008. Atlantic hurricane season of 2005. Mon. Weather Rev. 136, 1109–1173.
Blake, E.S., Rappaport, E.N., Jarrell, J.D., Landsea, C., 2005. The deadliest, costliest, and most intense United States tropical cyclones from 1851 to 2004 (and other frequently requested hurricane facts). In. Miama: National Hurricane Center, NOAA.
Boose, E.R., Foster, D.R., Fluet, M., 1994. Hurricane impacts to tropical and temperate forest landscapes. Ecol. Monogr. 64, 369–400.
Boose, E.R., Serrano, M.I., Foster, D.R., 2004. Landscape and regional impacts of hurricanes in Puerto Rico. Ecol. Monogr. 74, 335–352.
Boutet, J.C., Weishampel, J.F., 2003. Spatial pattern analysis of pre-and post-hurricane forest canopy structure in North Carolina, USA. Landscape Ecol. 18, 553–559.
Brun, J., Barros, A.P., 2013. Vegetation activity monitoring as an indicator of eco-hydrological impacts of extreme events in the southeastern USA. Int. J. Remote Sens. 34, 519–544.
Burslem, D., Whitmore, T.C., Brown, G.C., 2000. Short-term effects of cyclone impact and long-term recovery of tropical rain forest on Kolombangara, Solomon Islands. J. Ecol. 88, 1063–1078.
Chambers, J.Q., Fisher, J.I., Zeng, H., Chapman, E.L., Baker, D.B., Hurtt, G.C., 2007. Hurricane Katrina's carbon footprint on U.S. Gulf Coast Forests. Science 318, 1107.
Chapman, E.L., Chambers, J.Q., Ribbeck, K.F., Baker, D.B., Tobler, M.A., Zeng, H., White, D.A., 2008. Hurricane Katrina impacts on forest trees of Louisiana's Pearl River basin. Forest Ecol. Manag. 256, 883–889.
Clark, J., Finco, M., Schwind, B., Megown, K., 2006, Rapid assessment of forest damage using multi-temporal Landsat TM imagery and high resolution aerial photography. In: 8th Annual Forest Inventory and Analysis Symposium, Monterey, California, pp. 16–19.
Cleveland, R.B., Cleveland, W.S., McRae, J.E., Terpenning, I., 1990. STL: a seasonal-trend decomposition. J. Off. Stat 6, 3–73.
Dahal, D., Liu, S., Oeding, J., 2015. The Carbon Cycle and Hurricanes in the United States between 1900 and 2011. Sci. Rep. 4 (1). https://doi.org/10.1038/srep05197.
Davi, H., Baret, F., Huc, R., Dufrêne, E., 2008. Effect of thinning on LAI variance in heterogeneous forests. Forest Ecol. Manag. 256, 890–899.
de Beurs, K.M., McThompson, N.S., Owsley, B.C., Henebry, G.M., 2019. Hurricane damage detection on four major Caribbean islands. Remote Sens. Environ. 229, 1–13.
Frangi, J.L., Lugo, A.E., 1991. Hurricane damage to a flood plain forest in the Luquillo Mountains of Puerto Rico. Biotropica 324–335.
Goetz, J.S., Fiske, J.G., Bunn, G.A., 2006. Using satellite time-series data sets to analyze fire disturbance and forest recovery across Canada. Remote Sens. Environ. 101, 352–365.
Hao, Z., Yuan, X., Xia, Y., Hao, F., Singh, V.P., 2017. An overview of drought monitoring and prediction systems at regional and global scales. B. Am. Meteorol. Soc. 98, 1879–1896.
Hu, T., Smith, R., 2018. The impact of Hurricane Maria on the vegetation of Dominica and Puerto Rico using multispectral remote sensing. Remote Sens.-Basel 10, 827.

Huete, A., Didan, K., Miura, T., Rodriguez, E.P., Gao, X., Ferreira, L.G., 2002. Overview of the radiometric and biophysical performance of the MODIS vegetation indices. Remote Sens. Environ. 83, 195–213.
Imbert, D., 2018. Hurricane disturbance and forest dynamics in east Caribbean mangroves. Ecosphere 9, e2231.
Imbert, D., Rousteau, A., Labbé, P., 1998. Ouragans et diversité biologique dans les forêts tropicales. L'exemple de la Guadeloupe. Acta Oecologica 19, 251–262.
Jian, J., Steele, M.K., Thomas, R.Q., Day, S.D., Hodges, S.C., 2018. Constraining estimates of global soil respiration by quantifying sources of variability. Global Change Biol. 24, 4143–4159.
Mostafiz, C., Chang, N., 2018. Tasseled cap transformation for assessing hurricane landfall impact on a coastal watershed. Int. J. Appl. Earth Obs 73, 736–745.
Landsea, C.W., Franklin, J.L., 2013. Atlantic hurricane database uncertainty and presentation of a new database format. Mon. Weather Rev. 141, 3576–3592.
Lee, J., Frankenberg, C., van der Tol, C., Berry, J.A., Guanter, L., Boyce, C.K., Fisher, J.B., Morrow, E., Worden, J.R., Asefi, S., 2013. Forest productivity and water stress in Amazonia: observations from GOSAT chlorophyll fluorescence. Proc. Roy. Soc. B: Biol. Sci. 280, 20130171.
Li, X., Xiao, J., 2019. A Global, 0.05-Degree product of solar-induced chlorophyll fluorescence derived from OCO-2, MODIS, and Reanalysis Data. Remote Sens.-Basel 11, 517.
McNulty, S.G., 2002. Hurricane impacts on US forest carbon sequestration. Environ. Pollut. 116 (2002), S17–S24.
Negrón-Juárez, R., Baker, D.B., Chambers, J.Q., Hurtt, G.C., Goosem, S., 2014. Multi-scale sensitivity of Landsat and MODIS to forest disturbance associated with tropical cyclones. Remote Sens. Environ. 140, 679–689.
Negrón-Juárez, R., Baker, D.B., Zeng, H., Henkel, T.K., Chambers, J.Q., 2010. Assessing hurricane-induced tree mortality in US Gulf Coast forest ecosystems. J. Geophys. Res. Biogeosci. 115.
Potter, C., 2014. Global assessment of damage to coastal ecosystem vegetation from tropical storms. Remote Sens. Lett. 5, 315–322.
Qiu, R., Han, G., Ma, X., Xu, H., Shi, T., Zhang, M., 2020. A comparison of OCO-2 SIF, MODIS GPP, and GOSIF Data from Gross Primary Production (GPP) estimation and seasonal cycles in North America. Remote Sens.-Basel 12, 258.
Ramsey, E.W., Rangoonwala, A., Middleton, B., Lu, Z., 2009. Satellite optical and radar data used to track wetland forest impact and short-term recovery from Hurricane Katrina. Wetlands 29, 66–79.
Ramsey, E.W., Chappell, D.K., Jacobs, D.M., Sapkota, S.K., Baldwin, D.G., 1998. Resource management of forested wetlands: hurricane impact and recovery mapped by combining Landsat TM and NOAA AVHRR data. Photogram. Eng. Remote Sens. 64, 733–738.
Ramsey, E.W., Hodgson, M.E., Sapkota, S.K., Nelson, G.A., 2001. Forest impact estimated with NOAA AVHRR and Landsat TM data related to an empirical hurricane wind-field distribution. Remote Sens. Environ. 77, 279–292.
Rogan, J., Schneider, L., Christman, Z., Millones, M., Lawrence, D., Schmook, B., 2011. Hurricane disturbance mapping using MODIS EVI data in the southeastern Yucatán, Mexico. Remote Sens. Lett. 2, 259–267.
Schaaf, C., Wang, Z., 2015, MCD43A4 MODIS/Terra + Aqua BRDF/Albedo Nadir BRDF Adjusted Ref Daily L3 Global - 500m V006, distributed by NASA EOSDIS Land Processes DAAC, https://doi.org/10.5067/MODIS/MCD43A4.006.
Schott, T., Landsea, C., Hafele, G., Lorens, J., Taylor, A., Thurm, H., Ward, B., Willis, M., Zaleski, W. (2019). The Saffir-Simpson Hurricane Wind Scale. https://www.nhc.noaa.gov/pdf/sshws.pdf.
Stanturf, J.A., Goodrick, S.L., Outcalt, K.W., 2007. Disturbance and coastal forests: A strategic approach to forest management in hurricane impact zones. Forest Ecol. Manag. 250, 119–135.
Svoboda, M., LeComte, D., Hayes, M., Heim, R., Gleason, K., Angel, J., Rippey, B., Tinker, R., Palecki, M., Stooksbury, D., 2002. The drought monitor. B. Am. Meteorol. Soc. 83, 1181–1190.
Tanner, E., Kapos, V., Healey, J.R., 1991. Hurricane effects on forest ecosystems in the Caribbean. Biotropica 513–521.
Vidon, P., Marchese, S., Rook, S., 2017. Impact of Hurricane Irene and Tropical Storm Lee on riparian zone hydrology and biogeochemistry. Hydrol. Process. 31, 476–488.
Wang, F., D'Sa, E.J., 2010. Potential of MODIS EVI in identifying hurricane disturbance to coastal vegetation in the northern Gulf of Mexico. Remote Sens.-Basel 2, 1–18.
Wang, S., Huang, C., Zhang, L., Lin, Y., Cen, Y., Wu, T., 2016. Monitoring and assessing the 2012 drought in the great plains: analyzing satellite-retrieved solar-induced chlorophyll fluorescence, drought indices, and gross primary production. Remote Sens.-Basel 8, 61.
Wang, W., Qu, J.J., Hao, X., Liu, Y., Stanturf, J.A., 2010. Post-hurricane forest damage assessment using satellite remote sensing. Agr. Forest Meteorol. 150, 122–132.
Wang, Z., Schaaf, C.B., Sun, Q., Shuai, Y., Román, M.O., 2018. Capturing rapid land surface dynamics with Collection V006 MODIS BRDF/NBAR/Albedo (MCD43) products. Remote Sens. Environ. 207, 50–64.
Wang, F., Xu, Y., 2009. Hurricane Katrina-induced forest damage in relation to ecological factors at landscape scale. Environ. Monit. Assess. 156, 491–507.
Wei, Z., Yoshimura, K., Wang, L., Miralles, D.G., Jasechko, S., Lee, X., 2017. Revisiting the contribution of transpiration to global terrestrial evapotranspiration. Geophys. Res. Lett. 44, 2792–2801.
Weinkle, J., Landsea, C., Collins, D., Musulin, R., Crompton, R.P., Klotzbach, P.J., Pielke, R., 2018. Normalized hurricane damage in the continental United States 1900–2017. Nature Sustainability 1, 808.
Xiao, J., Chevallier, F., Gomez, C., Guanter, L., Hicke, J.A., Huete, A.R., Ichii, K., Ni, W., Pang, Y., Rahman, A.F., 2019. Remote sensing of the terrestrial carbon cycle: a review of advances over 50 years. Remote Sens. Environ. 233, 111383.
Xuan, Z., Chang, N., 2014. Modeling the climate-induced changes of lake ecosystem structure under the cascade impacts of hurricanes and droughts. Ecol. Model. 288, 79–93.
Yang, J., He, Y., Aubrey, D.P., Zhuang, Q., Teskey, R.O., 2016. Global patterns and predictors of stem CO_2 efflux in forest ecosystems. Global Change Biol. 22, 1433–1444.
Yang, J., Pan, S., Dangal, S., Zhang, B., Wang, S., Tian, H., 2017. Continental-scale quantification of post-fire vegetation greenness recovery in temperate and boreal North America. Remote Sens. Environ. 199, 277–290.
Yang, J., Tian, H., Pan, S., Chen, G., Zhang, B., Dangal, S., 2018. Amazon drought and forest response: Largely reduced forest photosynthesis but slightly increased canopy greenness during the extreme drought of 2015/2016. Global Change Biol. 24, 1919–1934.
Yoshida, Y., Joiner, J., Tucker, C., Berry, J., Lee, J., Walker, G., Reichle, R., Koster, R., Lyapustin, A., Wang, Y., 2015. The 2010 Russian drought impact on satellite measurements of solar-induced chlorophyll fluorescence: insights from modeling and comparisons with parameters derived from satellite reflectances. Remote Sens. Environ. 166, 163–177.
Yuan, H., Dai, Y., Xiao, Z., Ji, D., Shangguan, W., 2011. Reprocessing the MODIS Leaf Area Index products for land surface and climate modelling. Remote Sens. Environ. 115, 1171–1187.
Zarco-Tejada, P.J., Berni, J.A., Suárez, L., Sepulcre-Cantó, G., Morales, F., Miller, J.R., 2009. Imaging chlorophyll fluorescence with an airborne narrow-band multispectral camera for vegetation stress detection. Remote Sens. Environ. 113, 1262–1275.
Zeng, H., Chambers, J.Q., Negron-Juarez, R.I., Hurtt, G.C., Baker, D.B., Powell, M.D., 2009. Impacts of tropical cyclones on U.S. forest tree mortality and carbon flux from 1851 to 2000. Proc. Natl. Acad. Sci. USA 106, 7888–7892.
Zhang, L., Qiao, N., Huang, C., Wang, S., 2019. Monitoring drought effects on vegetation productivity using satellite solar-induced chlorophyll fluorescence. Remote Sens.-Basel 11, 378.
Zimmerman, J.K., Covich, A.P., 2007. Damage and recovery of riparian Sierra palms after Hurricane Georges: influence of topography and biotic characteristics. Biotropica 39, 43–49.